A novel RNA motif for neomycin recognition

Mary G Wallis[1,2], Uwe von Ahsen[1], Renée Schroeder[1]* and Michael Famulok[2]

[1]Institut für Mikrobiologie und Genetik, Universität Wien, Dr Bohrgasse 9, A-1030 Wien, Austria and [2]Institut für Biochemie, Ludwig-Maximilians-Universität München, Würmtalstrasse 221, D-81375 München, Germany

Background: Antibiotics can interfere with RNA activity. Translation of RNA by the prokaryotic ribosome, self-splicing of group I introns, HIV replication and hammerhead ribozyme cleavage are inhibited by the aminoglycoside neomycin B. To explore the molecular basis by which small molecules such as antibiotics inhibit RNA function, we undertook an *in vitro* selection to obtain a variety of RNA molecules with the capacity to recognize neomycin.

Results: The majority of the RNA molecules selected to specifically bind neomycin share a region of nucleotide sequence homology. From chemical probing and covariations among different clones we show that in all sequences this region folds into a hairpin structure, which from footprinting and partial alkaline hydrolysis experiments is shown to be the neomycin-binding site. Neomycin is recognized with high affinity ($K_d \approx 100$ nM) and high specificity (>100-fold higher affinity for neomycin than for paromomycin).

Conclusions: The fact that RNAs containing the consensus sequence, as well as sequences that display variations within this region, specifically recognize neomycin suggests that a structural motif rather than a particular nucleotide sequence is required for neomycin recognition. We propose that a hairpin stem–loop structural motif, which might feature a widened major groove, may be a prerequisite for neomycin recognition. This structural pattern can be extrapolated to other natural neomycin-responsive RNAs.

Introduction

Aminoglycosides, as well as other families of antibiotics, are thought to disrupt several biological functions by directly interacting with RNA target sites. For example, neomycin B and related aminoglycosides such as paromomycin bind to the A site of the 16S ribosomal RNA, which harbours the decoding function, and cause mistranslation, disturbing the synthesis of the encoded protein [1]. Many of these aminoglycoside antibiotics were also found to inhibit group I intron self-splicing; neomycin B inhibits self-splicing at the same low micromolar concentration as found for disruption of ribosome function [2,3]. Another RNA target affected by neomycin B is the Rev-responsive element (RRE), a segment in HIV-1 RNA that binds to the Rev protein. Neomycin B binds specifically to the same region within the RRE that is recognized by Rev and thus inhibits viral replication. This RNA–protein interaction is inhibited by neomycin B at a concentration of 1 μM [4,5]. An RNA more recently identified as a target for neomycin B is the hammerhead ribozyme. The cleavage activity of the ribozyme is impeded by 13.5 μM neomycin B [6].

These RNA targets, with the exception of the ribosomal RNA, can discriminate between the structural analogues neomycin B and paromomycin (Fig. 1). Paromomycin, which differs from neomycin in the substitution of a single amino group with a hydroxyl group, is one [6] or two [2,3,5] orders of magnitude weaker at eliciting an inhibitory response. An oligoribonucleotide analog of the decoding site of the 16S ribosomal RNA binds

neomycin and paromomycin with equal affinity, however, mirroring the lack of discrimination of the ribosomal RNA [7].

No primary sequence homologies exist between these different RNAs. What, then, is being recognized by the antibiotics, or what is it that unites diverse RNAs as a common target? Changes in reactivity toward chemical attack in the presence of antibiotics suggested structural parallels between the recognition processes involved in decoding by the A site of the 16S ribosomal RNA [8] and in group I intron self-splicing [9]. Based on these results, a possible relationship between the mechanisms of splice-site selection and tRNA selection during decoding, which involves similar structural motifs recognized by antibiotics, has been proposed [10].

An oligoribonucleotide analogue of the decoding region of the 16S ribosomal RNA (rRNA) was shown to interact with antibiotics in a manner that mimicked the biologically relevant conformation of this A-site subdomain [7]. Similarly, for the RRE it was shown that neomycin protects some bases from chemical modification that are also strongly protected by Rev [5]. These bases are part of the core region within the RRE. Short structural analogues of this region were found to bind selectively to Rev, suggesting that these motifs are also likely to be sufficient for neomycin recognition [11].

Do all these different natural RNAs share common, yet unidentified structural motifs which make them a target for

---

*Corresponding author.

	R¹	R²	R³	R⁴	R⁵	R⁶
Neomycin B	NH₂	OH	H	CH₂NH₂	H	H
Paromomycin	OH	OH	H	CH₂NH₂	H	H
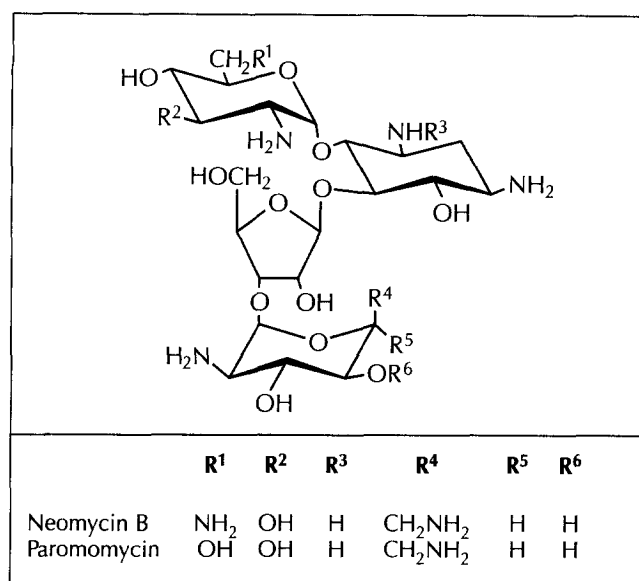
Fig. 1. Structure of the aminoglycoside antibiotics neomycin ($R^1 =$ $-NH_2$) and paromomycin ($R^1 = -OH$).

recognition by neomycin B? Using *in vitro* selection, we set out to obtain a series of short RNA sequences from a randomized pool that bind to neomycin B and allow a comparison with the natural neomycin-responsive RNAs. *In vitro* selection or SELEX [12–14] allows the screening of a large number of individual nucleic acid molecules for different functionalities (reviewed in [15–18]). Our aim was to isolate and characterize small RNA molecules which could interact with antibiotics specifically and with high affinity in solution. We sought to isolate recurring motifs recognized by antibiotics, in order to understand the minimal requirements of antibiotic–RNA interactions. Such information can then be used to help decipher known biological examples, which are often larger and less amenable to study. Characterization of these individual molecules revealed a novel motif that recognizes neomycin specifically and with high affinity.

Results

Novel neomycin-binding RNAs isolated by *in vitro* selection

RNA molecules having specific affinity for neomycin (Fig. 1) were isolated from a pool of RNA molecules with a random region of 74 nucleotides flanked by defined regions which enabled primer binding (total length 111 nucleotides). Initially the complexity of the pool was ~10^{15} different molecules. The pool was applied to a neomycin-derivatized agarose affinity column (neomycin concentration ~1 mM) followed by a buffer wash to remove non-specifically or weakly binding RNAs. Neomycin-binding RNAs were affinity-eluted with buffer containing 2.5 mM neomycin. To minimize enrichment of RNAs whose binding to neomycin involved contribution from the agarose matrix, the RNA molecules were affinity-eluted with free antibiotic in solution to guarantee a specific recognition of neomycin. The progress of the selection, as defined by the enrichment for neomycin-specific sequences, was monitored by determining the percentage of the input RNA eluted

from the neomycin–agarose with free antibiotic. Table 1 summarizes the evolution of the neomycin selection. Over the course of selection the stringency was increased by increasing the number of buffer washes prior to affinity elution with neomycin. Over the first three rounds of selection, as the number of buffer washes was progressively increased from 5 to 30 and then further to 50, the corresponding percentage of RNA eluted was selectively decreased from 12 % to 5.1 % and then to 0.22 %. During cycles three to six, where the number of buffer washes was held constant at 50, a 13-fold increase in the enrichment was seen from 0.22 % to 2.9 %. A dramatic increase was seen at cycle seven and a significant further increase at cycle eight. The selection was stopped when the elutable percentage of the neomycin-binding RNAs reached 55 %. Approximately 10^3 RNA molecules capable of binding neomycin were selected from the original pool of 10^{15}, suggesting that there are many possible sequence solutions to neomycin recognition.
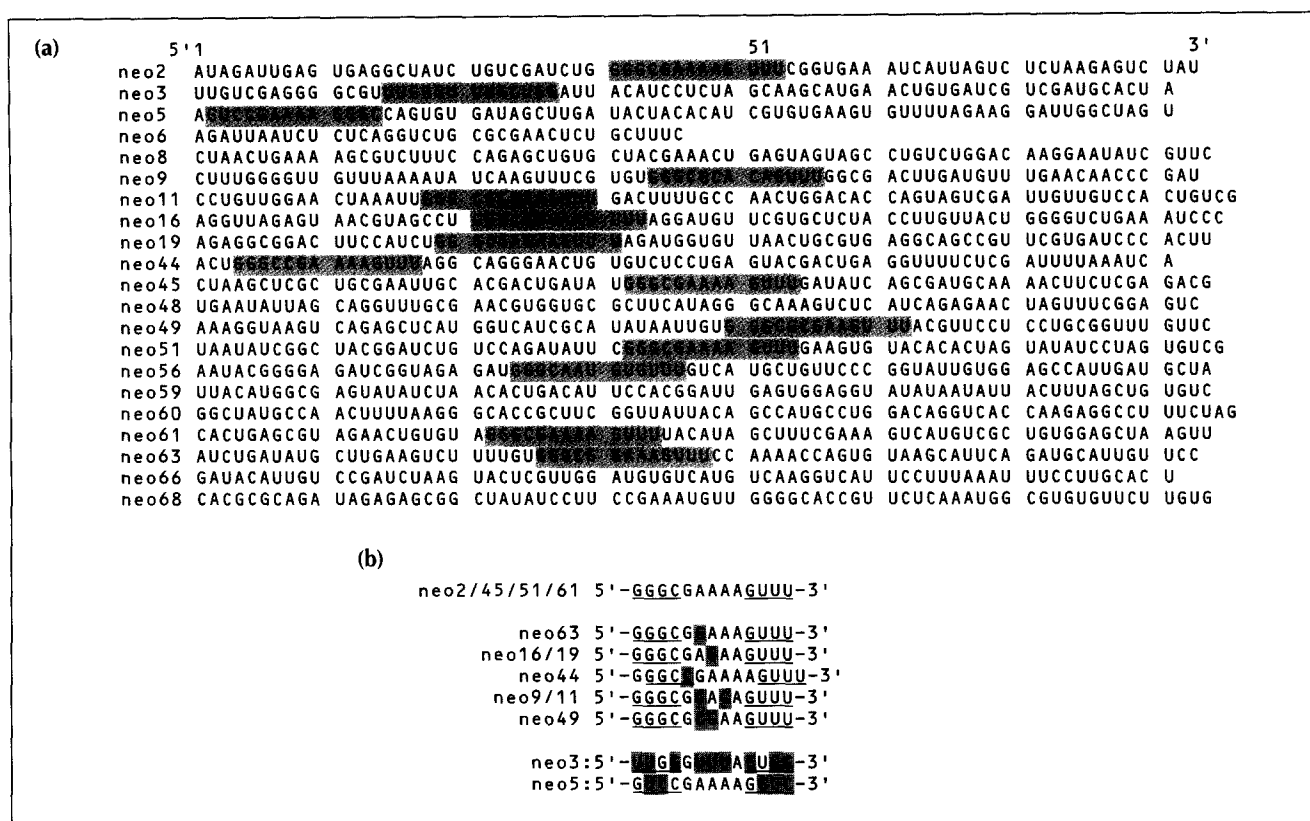
Sequence and structure analyses of individual neomycin-specific RNAs

To investigate the individual RNA species comprising the pool at the eighth selection cycle, the pool was cloned and 21 clones were sequenced. The random region sequences are shown in Fig. 2a. Despite the high specificity for neomycin, there was significant sequence variation among different clones. However, ~50 % of the RNAs contained a conserved 13-nucleotide consensus sequence, GGGCGNR-NAGUUU (where N is any nucleotide and R is a purine). Regions upstream and downstream of this consensus sequence can fold to form Watson–Crick base pairs. Folding of the individual full-length sequences having this motif with the Zuker program [19] presents this region of primary homology in a hairpin stem–loop structure. The stem varies both in sequence and in length and contains a conserved three-base-pair stretch of G:U wobble pairs. The loop sequences share the consensus GNRNA. The constant primer binding regions were not used in the structure prediction of this hairpin motif.

Table 1. Progressive enrichment of neomycin-specific RNAs.

Cycle	Buffer washes[a]	Affinity washes	% Input eluted[b]
1	5	2	12
2	30	2	5.1
3	50	2	0.22
4	50	2	0.40
5	50	2	1.6
6	50	2	2.9
7	30	2	24
8	30	2	55

The table summarizes the progressive stringency of selection. [a]Number of buffer washes before the neomycin-affinity wash. [b]RNA affinity-eluted with neomycin expressed as a percentage of the total RNA input.

(a)

```
            5'1                                                    51                                           3'
neo2   AUAGAUUGAG UGAGGCUAUC UGUCGAUCUG ▓▓▓▓▓▓▓▓▓CGGUGAA AUCAUUAGUC UCUAAGAGUC UAU
neo3   UUGUCGAGGG GCGU▓▓▓▓▓▓▓▓▓▓▓AUU ACAUCCUCUA GCAAGCAUGA ACUGUGAUCG UCGAUGCACU A
neo5   A▓▓▓▓▓▓▓▓▓▓▓▓▓CAGUGU GAUAGCUUGA UACUACACAU CGUGUGAAGU GUUUUAGAAG GAUUGGCUAG U
neo6   AGAUUAAUCU CUCAGGUCUG CGCGAACUCU GCUUUC
neo8   CUAACUGAAA AGCGUCUUUC CAGAGCUGUG CUACGAAACU GAGUAGUAGC CUGUCUGGAC AAGGAAUAUC GUUC
neo9   CUUUGGGGUU GUUUAAAAUA UCAAGUUUCG UGU▓▓▓▓▓▓▓▓▓GGCG ACUUGAUGUU UGAACAACCC GAU
neo11  CCUGUUGGAA CUAAAUU▓▓▓▓▓▓▓▓▓▓GACUUUUGCC AACUGGACAC CAGUAGUCGA UUGUUGUCCA CUGUCG
neo16  AGGUUAGAGU AACGUAGCCU ▓▓▓▓▓▓▓▓▓▓AGGAUGU UCGUGCUCUA CCUUGUUACU GGGGUCUGAA AUCCC
neo19  AGAGGCGGAC UUCCAUCU▓▓▓▓▓▓▓AGAUGUGU UAACUGCGUG AGGCAGCCGU UCGUGAUCCC ACUU
neo44  ACU▓▓▓▓▓▓▓▓▓▓▓AGG CAGGGAACUG UGUCUCCUGA GUACGACUGA GGUUUUCUCG AUUUUAAAUC A
neo45  CUAAGCUCGC UGCGAAUUGC ACGACUGAUA U▓▓▓▓▓▓▓▓▓▓▓GAUAUC AGCGAUGCAA AACUUCUCGA GACG
neo48  UGAAUAUUAG CAGGUUUGCG AACGUGGUGC GCUUCUAGG GCAAAGUCUC AUCAGAGAAC UAGUUUCGGA GUC
neo49  AAAGGUAAGU CAGAGCUCAU GGUCAUCGCA UAUAAUUGU▓▓▓▓▓▓▓▓▓ACGUUCCU CCUGCGGUUU GUUC
neo51  UAAUUACGGC UACGGAUCUG UCCAGAAUU C▓▓▓▓▓▓▓▓▓▓▓GAAGUG UACACACUAG UAUAUCCUAG UGUCG
neo56  AAUACGGGGA GAUCGGUAGA GAU▓▓▓▓▓▓▓▓▓GUCA UGCUGUUCCC GGUAUUGUGG AGCCAUUGAU GCUA
neo59  UUACAUGGCG AGUAUAUCUA ACACUGACAU UCCACGGAUU GAGUGGAGGU AUAUAAUAUU ACUUUAGCUG UGUC
neo60  GGCUAUGCCA ACUUUUAAGG GCACCGCUUC GGUUAUUACA GCCAUGCCUG GACAGGUCAC CAAGAGGCCU UUCUAG
neo61  CACUGAGCGU AGAACUGUGU A▓▓▓▓▓▓▓▓▓▓▓UACAUA GCUUUCGAAA GUCAUGUCGC UGUGGAGCUA AGUU
neo63  AUCUGAUAUG CUUGAAGUCU UUUGU▓▓▓▓▓▓▓▓CC AAAACCAGUG UAAGCAUUCA GAUGCAUUGU UCC
neo66  GAUACAUUGU CCGAUCUAAG UACUCGUUGG AUGUGUCAUG UCAAGGUCAU UCCUUUAAAU UUCCUUGCAC U
neo68  CACGCGCAGA UAGAGAGCGG CUAUAUCCUU CCGAAAUGUU GGGGCACCGU UCUCAAAUGG CGUGUGUUCU UGUG
```

(b)

```
neo2/45/51/61  5'-GGGCGAAAAGUUU-3'

        neo63  5'-GGGCG▓AAAGUUU-3'
     neo16/19  5'-GGGCGA▓AAGUUU-3'
        neo44  5'-GGGC▓GAAAAGUUU-3'
       neo9/11 5'-GGGCG▓A▓AGUUU-3'
        neo49  5'-GGGCG▓AAGUUU-3'

        neo3:5'-▓▓G▓G▓▓▓A▓U▓-3'
        neo5:5'-G▓▓CGAAAG▓▓-3'
```

Fig. 2. Nucleotide sequences of neomycin–agarose selected clones. **(a)** Sequences of 21 individual clones from the pool after the eighth cycle of the neomycin selection. The clone number is shown at the left-hand side. The sequences shown comprise only the 74 nucleotides that were random at the beginning of the selection. Nucleotides matching the 13-nucleotide consensus sequence and closely matching sequences are highlighted in green. **(b)** Consensus sequence of the motif recognized by neomycin. The most conserved region (13 nucleotides). Highlighted in orange are nucleotides differing from the most commonly occurring sequence, 5'-GGGC-GAAAAGUUU-3'. Of the consensus variations, the upper group comprises those sequences with minor deviations from this consensus, whereas the lower pair show more extensive divergence. The underlined nucleotides indicate putative base-pairing partners.

Other sequences, which might initially appear less closely related to this conserved motif due to significant sequence variation, are nonetheless intriguing for two reasons: (i) the clones still have the potential to form the proposed hairpin structure containing a five-membered loop, and (ii) the positions of the variations within this hairpin structure (Fig. 2b). Notable examples include clones neo3 and neo5. For clone neo5, significant variability is seen in the stem. The resulting hairpin structure has two of the G:U wobble base pairs replaced with G:C base pairs. Neo3 also shows sequence variations in both the loop and the stems; the hairpin structure nonetheless contains three G:U pairs and a G:C pair closing the loop. The presence of clones neo3 and neo5 in the selected sequences gives weight to this novel hairpin stem–loop structure. To test whether these sequence covariations indeed reflect our proposed secondary structure model, we analyzed a series of the selected sequences by chemical modification.

Footprinting the sites of interaction of neomycin with selected RNAs

We also used a second approach to localize the region of neomycin interaction within individual selected clones. Base-specific chemical probes were used (i) to investigate the solution structure of the RNAs and (ii) to

identify the neomycin binding site(s). RNA from representative clones of different sequence classes (see Fig. 2b) were incubated in the presence or absence of neomycin or paromomycin under the same conditions used in the selection procedure. Dimethyl sulfate (DMS), kethoxal or CMCT (1-cyclohexyl-3-(2-morpholinoethyl)-carbodiimide metho-p-toluene sulfonate) were subsequently added to modify bases specifically at accessible positions, as described previously [9,20]. DMS methylates adenine at position N1, cytosine at N3 and also the N7 position of guanine, kethoxal modifies the N1 and N2 positions of guanine and CMCT modifies the N1 and N3 of guanine and uracil, respectively. Positions of modification were determined by reverse transcription of probed RNAs. A typical autoradiograph showing the modification pattern of clone neo5 is shown in Figure 3a.

In the presence of 1 μM neomycin, several bases were clearly protected against modification by DMS or kethoxal. It is remarkable that these bases all fall into or around the conserved sequence motif described above. Little protection of the same bases was observed using a 100-fold higher concentration of the closely related antibiotic paromomycin. The kethoxal modification pattern of clone neo16 is shown in Figure 3b. Here, a
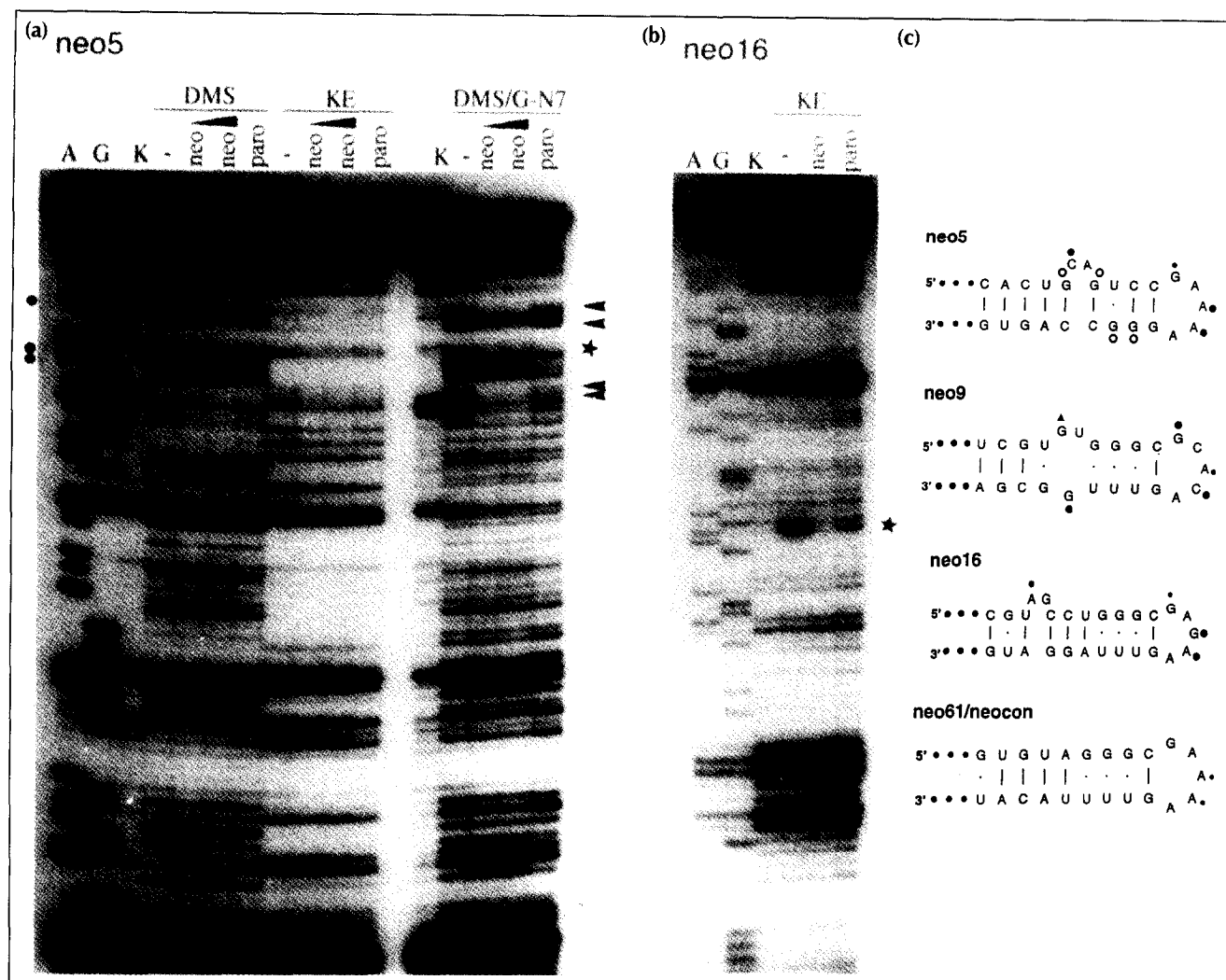
Fig. 3. Probing the structure of selected antibiotic binding RNAs in the presence of neomycin. **(a)** Modification pattern of clone neo5. The neomycin concentrations were 1 and 10 µM; the paromomycin concentration was 100 µM. Dots indicate protection at adenines and cytidines; stars and arrows indicate protection at guanine N1/N2 or N7 positions, respectively. K: control (no modification), – : no antibiotic, KE: kethoxal, DMS/G-N7: detection of modification at G-N7, A and G: dideoxy sequencing lanes. **(b)** Kethoxal modification pattern of clone neo16. Same abbreviations as in (a). The neomycin concentration was 1 µM and paromomycin was 100 µM. **(c)** Secondary structure representation of regions showing neomycin footprint from the clones tested in chemical probing experiments. Positions of protection or enhancement by neomycin at 1 µM are indicated. Large symbols represent complete protection, small symbols, weak protection. ● : protection by neomycin at Watson–Crick positions; ▲ : enhancement by neomycin at Watson–Crick positions; ○ : protection by neomycin at G-N7 positions.

similar pattern is observed: complete protection of an otherwize highly modified guanine in the presence of 1 µM neomycin (in addition to other bases in the hairpin motif, data not shown), and less protection using 100 µM paromomycin. This protected guanine lies in the middle of the conserved five-membered loop described above (Fig. 3c).

Two more clones from other classes of selected RNAs (neo9 and neo61) were tested for binding of antibiotics by chemical probing. Again, the neomycin footprint was located solely within the conserved motif with at least 100-fold discrimination compared to paromomycin (data not shown). The secondary structure and the neomycin protection patterns of the four clones are summarized in Figure 3c. It is interesting to note that part of the footprint pattern was always located at the third and fourth

nucleotides of the loop, independent of which nucleotide was present at this position.

The principal stem–loop structure suggested by sequence comparison was corroborated by the modification pattern of the RNAs in the absence of antibiotics. In addition, the chemical probing analysis suggests that the stem contains bulged nucleotides, some of which become strongly protected against modification by neomycin binding.

Finally, the clone neo3 was tested because of the strong divergence in the loop region (three uridines) from the consensus sequence. Because of strong stops of the reverse-transcribed RNA in the loop region we were unable to inspect this part of the motif (by CMCT modification). However, a strong neomycin-induced

footprint of a bulged cytidine seven nucleotides upstream of the loop suggests that the binding region for neomycin is indeed localized in this region of the sequence (compare Fig. 2).

The strength of neomycin binding to the neo5 RNA was determined by titration of neomycin before DMS modification. The strength of protection of the two consecutive adenines in the loop region at neomycin concentrations between 1 μM and 50 nM was measured by quantifying the radioactivity in the respective bands with a Phosphorimager. In Figure 4, showing the graph of peak intensity versus neomycin concentration, it can be seen that the peak does not further level off at concentrations higher than 0.5 μM neomycin, where it reaches saturation. Samples showing a linear relationship between peak intensity and neomycin concentration were used for a regression analysis to estimate the dissociation constant (see inset Fig. 4). The K_d of neomycin to clone neo5 was determined to be 115 ± 25 nM. From visual inspection of autoradiographs from other chemical modification experiments we estimated the K_d of neomycin to be in the same range as that for the other footprinted clones.

Localization of the minimum neomycin-interaction site
As a first step towards ascertaining whether this putative motif was sufficient for neomycin binding in solution, a shortened version of one of the clones (neo61) was designed, taking into consideration the semi-conserved consensus sequence, to make a DNA template of reduced size (27 nucleotides in the 'random positions' compared with the original 74, giving an overall RNA length of 64 nucleotides including primer sites). The RNA resulting from this template is referred to as 'neocon'. The footprinting data for this smaller RNA reflected the pattern observed for the parent sequence neo61 (Fig. 3c) and confirmed the stem–loop structure. Furthermore, this
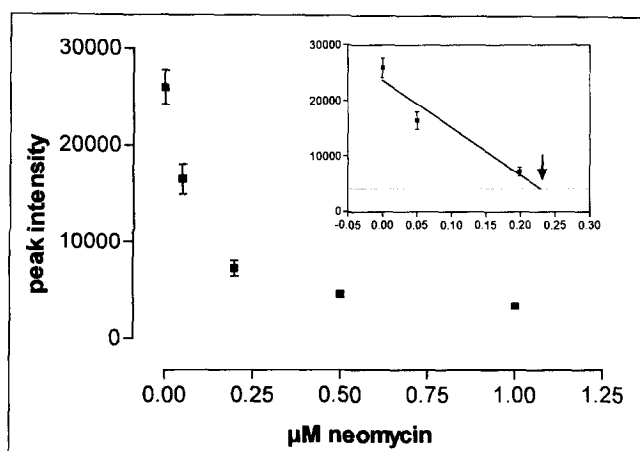
Figure 4. Quantification of protection against chemical modification of two consecutive adenines in the neo5 loop (see Figs 3a,c) by neomycin. The peak intensity of the two adenines (mean value with error bars) by DMS modification reaches background at 0.5 μM neomycin. The inset shows the same graph with an expanded X-axis and a linear regression reaching the saturation level (dotted line) at ~0.23 μM (see arrow). The K_d of neomycin binding to neo5 was inferred to be 115 ± 25 nM.

sequence had binding and elution characteristics which compared favourably with the parent sequence and other full-length neomycin-binding clones (data not shown).

To localize the antibiotic-recognition site within these selected sequences by an independent approach in addition to footprinting, and to determine whether the consensus region and resulting putative stem–loop structure were solely responsible for neomycin binding, we subjected end-labelled RNA from the four clones tested in the footprinting approach (neocon, neo5, neo9 and neo16) to partial alkaline hydrolysis. The idea was to generate RNA pools of the four individual sequences which encompassed all possible lengths between one nucleotide and the full-length RNA. These pools were tested for their abilities to bind to the neomycin column and to elute specifically with neomycin. The minimum length of RNA which is required for binding and elution by neomycin could thus be determined.

The 5' or 3' end-labelled, partially hydrolyzed pools from individual clones were applied to the neomycin–agarose column under the same conditions as in the initial sequence-selection procedure. After the buffer wash, the RNA was affinity-eluted with neomycin, precipitated and subjected to polyacrylamide gel electrophoresis, in parallel with non-selected, partially hydrolyzed RNA of the same pool and T_1-digested RNA, for sequence determination. As can be seen in Figure 5a,b (for either 5'-labelled or 3'-labelled RNA), there was always a certain sub-population of small RNAs that was unable to bind. By using either 5' or 3' end-labelled RNA, the nucleotides that can be removed from 3' or 5' ends of the RNA, respectively, without affecting binding can be determined to single-nucleotide resolution.

A graphical presentation of the nucleotides that could not be removed without affecting neomycin recognition and elution is shown in Figure 5c. The region that was found to be required for neomycin recognition in these experiments was identical to the region identified by sequence comparison and footprinting of the full-length RNAs. Taken together, these results suggest that this hairpin motif is sufficient for neomycin recognition. The total length necessary for binding of the individual clones was between 20 and 22 nucleotides, with the exception of clone neo9 which required a length of 36 nucleotides. Interestingly, some RNAs longer than the minimal ones seem to be counter-selected, as can be seen from the gaps in the lanes for the selected RNAs. It is possible that certain free ends might interfere with the crucial stem–loop structure, for example by base-pairing to the loop. Further characterization, including NMR analysis (M. Kochoyan, personal communication) of these short RNAs are currently under way.

Specific recognition of neomycin
To show that the affinity of the *in vitro* selected RNA molecules was specific for neomycin we tested the ability of individual clones to bind neomycin and a
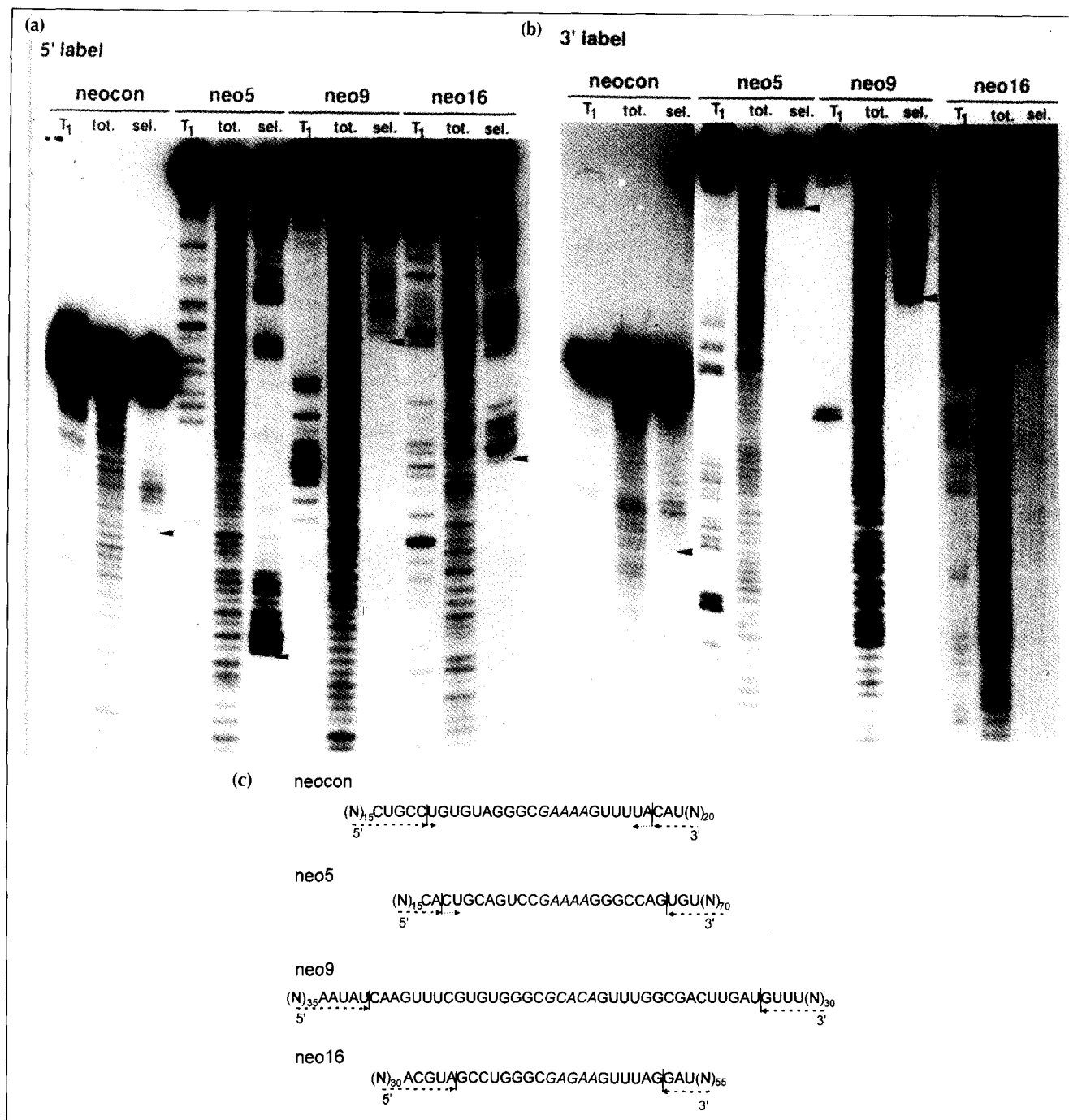
Fig. 5. Determination of length requirement for neomycin binding. Autoradiograph showing **(a)** 5'-labelled, or **(b)** 3'-labelled, partially-hydrolyzed RNAs from individual clones which were capable of binding to and eluting from neomycin–agarose (lanes labelled as 'sel'). Unselected ('tot') and T1-digested (non-hydrolyzed, lanes labelled as 'T1') RNAs were run in parallel. An arrow indicates the position from which further removal of nucleotides prevented neomycin recognition. **(c)** Summary diagram of the minimum neomycin-binding sequences as determined by selection of partially hydrolyzed RNAs. The loop region is shown in italics. Dotted arrows indicate nucleotides that can be removed while retaining neomycin-binding capacity.

closely related analogue, paromomycin (Fig. 1, $R_1 =$ $-NH_2$ and $-OH$, respectively) since this conservative structural substitution results in a dramatic difference in activity [3,5,6].

Individual clones were applied to the neomycin–agarose column and the RNA was affinity-eluted with antibiotic. Thus a competition exists between antibiotic (either neomycin or paromomycin) in solution and immobilized

neomycin on the column. The ability of neomycin or paromomycin to affinity-elute RNA was compared in two ways: the percentages of RNA eluted were compared for a given antibiotic concentration (see Table 2), and the antibiotic concentrations required to elute a given percentage of RNA were compared (data not shown). Although these structural analogues are extremely similar, a strong preference for neomycin over paromomycin can be seen. This discriminatory

Table 2. Antibiotic affinity and homologue discrimination for clone neo5.

Antibiotic concentration	Neomycin[a]	Paromomycin[a]
250 μM	54 %	0.6 %
25 μM	48 %	ND

Effect of varying the concentration or type of antibiotic on elution of RNA from a neomycin–agarose column.
[a]Output counts per minute (cpm) as a percentage of the input cpm for two affinity washes. ND, not determined.

behaviour, which was not selected for, was also seen in the chemical modification analyses in which paromomycin protected the selected RNAs only at a concentration 100-fold higher than neomycin.

Magnesium dependence and metal specificity analyses

For neomycin, the sensitivity of group I intron self-splicing to antibiotic was shown to increase as the concentration of Mg^{2+} ions decreased [21]. A similar competitive effect of Mg^{2+} on neomycin inhibition was found for the hammerhead ribozyme [22]. These observations are consistent with the fact that at neutral pH the antibiotic is positively charged [23]. We investigated the possible electrostatic component of this interaction by monitoring the ability of RNAs to recognize neomycin under varying Mg^{2+} ion concentrations and in the presence of different divalent ions.

Individual RNAs were applied to a neomycin–agarose column, washed with buffer to remove RNAs that did not specifically bind to the antibiotic and affinity-eluted with neomycin in the same buffer. The buffers differed only in the concentration of $MgCl_2$ in the range from 0–20 mM. Figure 6, which shows the effect of varying the concentration of divalent magnesium ions on the specific elution of RNA with neomycin, depicts the cumulative output RNA expressed as a percentage of

the input RNA plotted as a function of the fraction number for the clone neo5. This clearly demonstrates the effect on both RNA binding to neomycin immobilized on the agarose as well as free in solution. The elution profiles from fractions one to ten (buffer wash) represent the effect of Mg^{2+} ions on the binding of RNA to the neomycin coupled to the agarose, whereas in fractions 11 to 15 (affinity wash) the effect is on the ability of the RNA to recognize free neomycin in solution. It can be seen that increasing the concentration of Mg^{2+} ions in the buffer decreases the affinity of the RNA for the agarose-bound neomycin. The ability of neomycin to elute bound RNA from the column shows a maximum at ~5–10 mM Mg^{2+}. In the absence of divalent Mg ions some RNA can still be eluted with neomycin. The elution profiles of other clones (data not shown) show a similar response to the effect of varying Mg^{2+} concentration on binding to neomycin on the column. The optimum concentration for solution binding of neomycin, however, varies with different sequences. These results indicate either that Mg^{2+} competes with neomycin in the interaction with RNA, or that at higher magnesium concentrations a different RNA structure is formed which does not allow neomycin recognition. Note that the original selection conditions included 5 mM $MgCl_2$.

The hypothesis that neomycin and magnesium directly compete for binding to RNA was investigated by a footprinting experiment with the neo5 clone in the absence of magnesium ions. The modification pattern as well as the neomycin protections were found to be the same as in the experiment including 5 mM Mg^{2+}, indicating that the structure formation does not depend on Mg^{2+} ions. If magnesium competes with neomycin for the RNA, we would expect a much stronger footprint in the absence than in the presence of magnesium ions. This was not the case (data not shown). A more detailed quantitative analysis is required to address this question; it seems, however, that the interaction of neomycin with
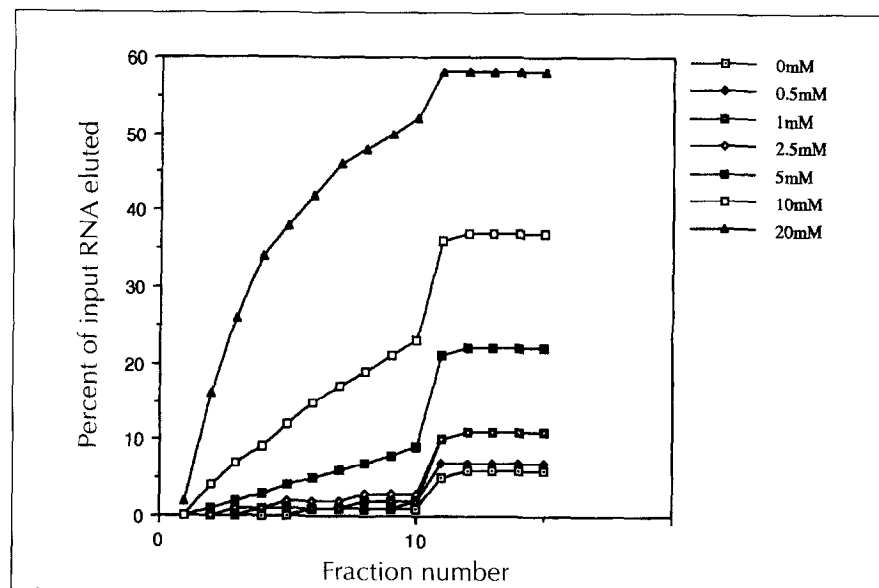
Fig. 6. Magnesium concentration (0–20 mM Mg^{2+}) dependence elution profile for neo5. Cumulative output cpm are expressed as a percentage of the input cpm. Internally labelled RNA was specifically affinity-eluted with neomycin (2.5 mM, fractions 11–15) from neomycin–agarose.

our RNAs cannot solely be explained by a competitive electrostatic interaction.

Finally, the effect of varying the type of divalent metal ion present in solution (while maintaining the concentration at 5 mM) upon the ability of individual RNA molecules to bind neomycin was also investigated (data not shown). Mg^{2+} and Ca^{2+} ions show very similar profiles. Both types of ions are able to mediate neomycin binding on the column and in solution. Mn^{2+} ions, however, are not; in the presence of manganese the RNA appears to be unable to assume a structure able to recognize agarose-bound neomycin.

Discussion

Eight rounds of *in vitro* selection allowed the enrichment of an RNA pool, originally containing $\sim 10^{15}$ different molecules, for RNAs specifically binding neomycin. Although there is considerable variability at the level of primary structure, more than 50 % of the sequences share a similar secondary structure, namely a hairpin whose stem is 'loosened' by the presence of G:U base pairs and which includes an asymmetric bulge. Chemical modification and partial alkaline hydrolysis analyses confirmed this structure and defined this novel stem–loop motif as the neomycin B binding site. From chemical modification analysis it was found that other sequences from our selection which differed from the consensus sequence also harboured this motif, and that variations in sequence are tolerated for neomycin recognition. It is plausible that in those sequences which lack the consensus sequence (see Fig. 2a) a similar motif is present but currently escapes our attention. Neomycin binds with high affinity ($K_d \approx 100$ nM) and high specificity (affinity for neomycin is >100-fold higher than for paromomycin). The neomycin-recognition properties of selected individual sequences were addressed with respect to various metal ion conditions. The optimum Mg^{2+} concentration for neomycin binding in solution varied depending on the individual RNA. Furthermore, Ca^{2+} ions were also able to substitute for Mg^{2+}.

RNA structures recognized by aminoglycoside antibiotics

Recently, *in vitro* selected RNAs with affinity for other aminoglycoside antibiotics, kanamycin A, lividomycin [24] and tobramycin [25], have been selected from random-sequence pools. Unlike the neomycin selection, the kanamycin A and lividomycin selections did not result in the isolation of any predominant sequence or structural feature. Similarly, the selection of tobramycin-binding RNAs under conditions of low stringency revealed no obvious consensus sequence. At high stringencies, however, two partially homologous consensus sequences were observed which are predicted to form stem–loop regions, possibly presenting a bulge. The binding sites of the antibiotics were not further determined.

The fact that our *in vitro* selected RNAs specifically recognize neomycin despite consensus-sequence variations, taken together with the observation that natural neomycin-responsive RNAs contain no sequence homology, leads us to conclude that it is predominantly structure, or molecular shape, that is crucial for neomycin recognition. Perhaps the most noticeable feature of our selected neomycin-binding RNA motif is the adjacent G:U wobble base pairs and the presence of an internal bulge in the majority of the selected sequences. An X-ray structural analysis of an RNA double helix [26] identified a widened major groove originating from alternating G:U and C:U base pairs contained in this helix. A very similar structural motif was identified in one of the natural neomycin-responsive RNA sequences, the core region of the RRE [4,11,27]. This region consists of at least two non-canonical Watson–Crick base pairs which lead to a widening of the major groove in the otherwise regular A-type helix of the flanking regions. Just like our selected motifs, the RRE core also contains internal bulges which are important for Rev and possibly also for neomycin binding. Perhaps this motif can be extrapolated to the decoding site of the 16S rRNA since it also presents an asymmetric bulged helix [28]. Several other examples of distorted or irregular helices featuring widened major grooves have been reported ([29] and references therein). The irregular structure of the eukaryotic 5S rRNA loop E results from uncommon base pairs such as G:A and the reverse-Hoogsteen configuration of A:U [30]. The sarcin/ricin loop structure is also stabilized by several non-Watson–Crick pairings [31].

From these analyses we conclude that the G:U pairs in our selected motifs, in addition to an asymmetric bulge, are likely to lead to a widened major groove formed by the helix in the hairpin. Furthermore, the protection pattern at G–N7 positions (positions that are located in the major groove of an A-type helix) can be found in all RNA molecules sensitive to neomycin B that have been footprinted [5,7–9]. One explanation for the G–N7 footprint is that it results from a direct contact with neoymcin which might require a widened major groove and would explain why the 'loosened stem' of the consensus motif is an important feature of the sequences isolated from our neomycin selection. This recognition element, however, may also include an as yet undefined sequence component since the majority of the selected sequences share a 13-nucleotide consensus region. Other *in vitro* selections show that many sequence solutions to aminoglycoside antibiotic binding appear to exist [24,25]. Our studies suggest, however, that a crucial factor for antibiotic recognition lies at the structural level. This may also hold true for these other selected sequences.

We have gained an insight into the RNA structural requirements for neomycin recognition which might be common to other neomycin-targeted RNAs. Many RNAs would fit these recognition criteria, which require further refinement. Additionally, for the naturally occurring neomycin-responsive RNAs a further constraint on RNA structure may be imposed at the functional level.

Significance

RNA molecules of diverse sequence and function can be inhibited by a single type of antibiotic molecule. To explore the molecular basis for the recognition of small molecules by RNAs, we undertook an *in vitro* selection to obtain a variety of RNA molecules with the capacity to recognize neomycin specifically and with high affinity. These RNAs present a consensus sequence which folds into a hairpin motif which includes a GNRNA loop, the stem of which might feature a widened major groove due to the presence of G:U base pairs and an asymmetric bulge. Three independent lines of evidence, sequence comparison, footprinting and partial alkaline hydrolysis experiments, identified this novel stem–loop motif as the neomycin-binding site. This structure, while novel, nonetheless contains features which we propose to be common to neomycin recognition since structural similarities can be identified in other neomycin targets. Thus *in vitro* selection has allowed us to gain an understanding of the minimal requirements of antibiotic–RNA interactions and to identify a structural motif that may be common to natural neomycin-responsive RNA targets.

Materials and methods

Materials

Neomycin sulphate (90–95 % neomycin B, balance neomycin C, a stereoisomer at the C_1 position of the B ring) and epoxy-activated Sepharose were purchased from the Sigma Chemical Company and Pharmacia Biotech, respectively. Hydrated metal chlorides were from Merck.

In vitro *selection: general molecular biology and random pool construction*

Reverse transcription, polymerase chain reaction amplification and transcription, cloning (pGem3Z vector, Promega) and sequencing were performed as reported elsewhere [32]. The original random-sequence RNA pool was synthesized as described previously [32]. For the first round of selection, approximately four pool equivalents were used.

Neomycin affinity chromatography selection procedure

The selection was performed with modifications to a previously described protocol [32]. ^{32}P-labelled RNA (16.6 nmol in the initial selection) in selection buffer (5 mM $MgCl_2$, 50 mM Tris-HCl pH 7.6, 250 mM NaCl) was applied to a 1 ml neomycin–agarose column. The agarose was derivatized following the manufacturer's recommended procedures. Neomycin was covalently coupled at ~1 mM, assuming a coupling efficiency of 50 %. The neomycin column was washed with selection buffer (buffer wash) before specifically bound RNAs were eluted by the addition of two column volumes of 2.5 mM neomycin in selection buffer (affinity wash). In the initial selection round the RNA was end-labelled, thereafter it was internally labelled. To minimize enrichment of RNA molecules not specifically recognising neomycin but binding also the agarose matrix, three precautions were taken. First, 1 mole-equivalent of unlabelled

tRNA (from brewer's yeast, Boehringer Mannheim GmbH) was added to the random sequence labelled RNA for the affinity-chromatography selection, and second, before the neomycin-column the RNA was passed over a glycine–agarose (0.5 ml, derivatized at 3 mM) precolumn which was washed, with one column volume only, directly onto the neomycin-affinity column. Third, the RNAs were eluted with free neomycin in solution. It is anticipated that the immobilized neomycin will exist as a heterogeneous population since this aminoglycoside antibiotic presents several functional groups with the potential to form a covalent linkage to the agarose matrix. However, specific elution of the RNA molecules with neomycin in solution ought to minimize the possibility of multiple recognition of this same molecule bound to the column. The eluted neomycin-specific RNA was ethanol-precipitated using glycogen as a carrier, converted to DNA and amplified by PCR, PAGE-purified and transcribed. This set of procedures constituted one selection cycle and the resulting purified RNA was the input for the subsequent round of selection.

Antibiotic affinity and discrimination, and metal dependence and selectivity

Tests for antibiotic affinity and discrimination, or metal dependence and selectivity were carried out using on average 0.1–1 µg of ^{32}P internally labelled RNA. The RNA was applied to a 1 ml neomycin–agarose column (derivatized at ~1mM), washed with selection buffer and specifically eluted with antibiotic in this buffer, as described above for the selection procedure. For the antibiotic-affinity experiments the buffer used was the standard selection buffer (5 mM $MgCl_2$, 50 mM Tris-HCl pH 7.6, 250 mM NaCl); the concentration of neomycin in the buffer varied only during affinity-elution, generally between 2.5 mM and 25 µM, as indicated in the text and in Table 2. The selection buffer was also employed for the metal dependence elution experiments, except that the Mg^{2+} concentration was varied over the range 0–20 mM (see Fig. 6). The concentration of neomycin in the affinity wash was always 2.5 mM under conditions of varying metal. The metal selectivity experiments similarly used the selection buffer except that the Mg was substituted with 5 mM of either Ca or Mn. Note that in addition the Mn-selection buffer contained 2.5 mM dithiothreitol. Fractions (one column volume) were quantitated by Cerenkov scintillation counting.

Selection of partially hydrolyzed RNAs

Individual clones (neocon, neo5, neo9 and neo16) were ^{32}P 5' or 3' end-labelled and subjected to partial alkaline hydrolysis. End-labelling was performed as described previously by the manufacturers of T4 RNA ligase (Boehringer Mannheim GmbH) and PNKinase (New England Biolabs). Alkaline hydrolysis was initiated by addition of the same volume of 50 mM $NaHCO_3$ (pH 8.5) to end-labelled RNA (in water) in the presence of 1.5 µg tRNA as carrier. Samples were incubated for 10 min at 90 °C and subsequently precipitated. The RNA was applied to neomycin–agarose (1 mM, 1 ml) and affinity-eluted with neomycin (0.25 mM in selection buffer, five column volumes) after removal of non-specific binding molecules with buffer (ten column volumes). The first and second neomycin affinity washes corresponded to 85–95 % of the elutable RNA at this neomycin concentration, hence only these two fractions were precipitated. Thus we obtained partially hydrolyzed RNA still capable of neomycin recognition. These molecules, sub-populations of

four full-length clones, were analyzed by electrophoresis on an 8 % polyacrylamide gel.

Chemical modification experiments

In vitro transcribed and gel-eluted RNA was activated in 2x binding buffer for 1.5 min at 56 °C, and subsequently transferred to 20 °C. 1x binding buffer (5 mM $MgCl_2$, 200 mM NH_4Cl, 80 mM K-cacodylate pH 7.4) and incubation temperature (20 °C) were chosen to be similar to selection conditions.

RNA (~1–5 pmole per sample) was preincubated with antibiotic for 15 min at 20 °C in 1x binding buffer in a 50 µl probing volume. Samples were transferred to ice and the modification agent was added and incubated for 10–15 min at 20 °C. For DMS modification, 1 µl 1:10 (in ethanol) diluted DMS was added, for kethoxal, 1 µl of 1:5 diluted kethoxal stock solution (37 mg ml⁻¹) was used, and for CMCT (1-cyclohexyl-3-(2-morpholinoethyl)-carbodiimide metho-*p*-toluene sulfonate) modification, 10 µl of a 34 mg ml⁻¹ solution (in binding buffer) was added in a 50 µl total probing volume.

After precipitation (in the presence of 10 µg glycogen), samples were dissolved in H_2O (or 25 mM K-borate pH 7.0 for kethoxal modified samples) and stored at –20 °C. Detection of modified positions by primer extension and polyacrylamide gel electrophoresis was performed as described previously [9,20].

References

1. Cundliffe, E. (1990). Recognition sites for antibiotics within rRNA. In *The Ribosome.* (Hill, W.E. *et al.*, eds), pp. 479–490, American Society of Microbiology, Washington.
2. von Ahsen, U., Davies, J. & Schroeder, R. (1991). Antibiotic inhibition of group I ribozyme function. *Nature* **353**, 368–370.
3. von Ahsen, U., Davies, J. & Schroeder, R. (1992). Non-competitive inhibition of group I intron RNA self-splicing by aminoglycoside antibiotics. *J. Mol. Biol.* **226,** 935–941.
4. Bartel, D.P., Zapp, M.L., Green, M.R. & Szostak, J.W. (1991). HIV-1 *rev* regulation involves recognition of non-Watson–Crick base pairs in viral RNA. *Cell* **67**, 529–536.
5. Zapp, M.L., Stern, S. & Green, M.R. (1993). Small molecules that selectively block RNA binding of HIV-1 Rev protein inhibit *rev* function and viral production. *Cell* **74**, 969–978.
6. Stage, T.K., Hertel, K.J. & Uhlenbeck, O.C. (1995). Inhibition of the hammerhead ribozyme by neomycin. *RNA* **1**, 95–101.
7. Purohit, P. & Stern, S. (1994). Interactions of a small RNA with antibiotic and RNA ligands of the 30S subunit. *Nature* **370**, 659–662.
8. Moazed, D. & Noller, H.F. (1987). Interaction of antibiotics with functional sites in 16S ribosomal RNA. *Nature* **327**, 389–394.
9. von Ahsen, U. & Noller, H.F. (1993). Footprinting the sites of interaction of antibiotics with catalytic group I intron RNA. *Science* **260**, 1500–1503.
10. Schroeder, R., Streicher, B. & Wank, H. (1993). Splice-site selection and decoding: are they related? *Science* **260**, 1443–1444.
11. Leclerc, F., Cedergreen, R. & Ellington, A.D. (1994). A three-dimen-

sional model of the Rev-binding element of HIV-1 derived from analyses of aptamers. *Nat. Struct. Biol.* **1**, 293–300.
12. Ellington, A.D. & Szostak, J.W. (1990). *In vitro* selection of RNA molecules that bind specific ligands. *Nature* **346**, 818–822.
13. Tuerk, C. & Gold, L. (1990). Systematic evolution of ligands by exponential enrichment: RNA ligands to bacteriophage T4 DNA polymerase. *Science* **249**, 505–510.
13. Robertson, D.L. & Joyce, G.F. (1990). Selection *in vitro* of an RNA enzyme that specifically cleaves single-stranded DNA. *Nature* **344**, 467–468.
15. Ellington, A.D. (1994). Aptamers achieve the desired recognition. *Curr. Biol.* **4**, 427–429.
16. Klug, S.J. & Famulok, M. (1994). All you wanted to know about SELEX. *Mol. Biol. Reports* **20**, 97–107.
17. Gold, L., *et al.*, & Tasset, D. (1993). RNA: the shape of things to come. In *The RNA World.* (Gesteland, R.F. & Atkins, J.F., eds), pp. 497–509, Cold Spring Harbor Laboratory Press, Cold Spring Harbor, New York.
18. Szostak, J.W. & Ellington, A.D. (1993). *In vitro* selection of functional RNA sequences. In *The RNA World.* (Gesteland, R.F. & Atkins, J.F., eds), pp. 511–533, Cold Spring Harbor Laboratory Press, Cold Spring Harbor, New York.
19. Zuker, M., Jaeger, J.A. & Turner, D.H. (1991). A comparison of optimal and suboptimal RNA secondary structures predicted by free energy minimization with structures determined by phylogenetic comparison. *Nucleic. Acids Res.* **19**, 2707–2714.
20. Stern, S., Moazed, D. & Noller, H.F. (1988). Structural analysis of RNA using chemical and enzymatic probing monitored by primer extension. *Methods Enzymol.* **164**, 481–489.
21. Hoch, I. (1995). Electrostatic interactions of antibiotics with the *td* group I intron RNA. Diploma thesis. University of Vienna.
22. Clouet D'Orval, B., Stage, K. & Uhlenbeck, O.C. (1995). Neomycin inhibition of the hammerhead ribozyme involves ionic interactions. *Biochemistry*, in press.
23. Botto, R.E. & Coxon, B. (1983). Nitrogen-15 nuclear magnetic resonance spectroscopy of neomycin B and related aminoglycosides. *J. Am. Chem. Soc.* **105**, 1021–1028.
24. Lato, S.M., Boles, A.R. & Ellington, A.D. (1995). *In vitro* selection of RNA lectins: using combinatorial chemistry to interpret ribozyme evolution. *Chemistry & Biology* **2**, 291–303.
25. Wang, Y. & Rando, R.R. (1995). Specific binding of aminoglycoside antibiotics to RNA. *Chemistry & Biololgy* **2**, 281–290.
26. Holbrook, S.R., Chaejoon, C., Tinoco, Jr I. & Kim, S.-H. (1991). Crystal structure of an RNA double helix incorporating a track of non-Watson–Crick base pairs. *Nature* **353**, 579–581.
27. Battiste, J.L., Tan, R., Frankel, A.D. & Williamson, J.R. (1994). Binding of an HIV Rev peptide to Rev responsive element RNA induces formation of purine–purine base pairs. *Biochemistry* **33**, 2741–2747.
28. Gutell, R.R. (1994). Collection of small subunit (16S- and 16S-like) ribosomal RNA structures: 1994. *Nucleic Acids Res.* **22**, 3502–3507.
29. Wyatt, J.R. & Tinoco, Jr I. (1993). RNA structural elements and RNA function. In *The RNA World.* (Gesteland, R.F. & Atkins, J.F., eds), pp. 465–496, Cold Spring Harbor Laboratory Press, Cold Spring Harbor, New York.
30. Wimberly, B., Varani, G. & Tinoco, Jr I. (1993). The conformation of loop E of eukaryotic 5S ribosomal RNA. *Biochemistry* **32**, 1078–1087.
31 Szewczak, A.A. & Moore, P.B. (1995). The sarcin/ricin loop, a modular RNA. *J. Mol. Biol.* **247**, 81–98.
32. Famulok, M. (1994). Molecular recognition of amino acids by RNA-aptamers: an L-citrulline binding RNA motif and its evolution into an L-arginine binder. *J. Am. Chem. Soc.* **116**, 1698–1706.